Mechanical Properties and Superstructure of Isotactic Polypropylene Fibers Prepared by Continuous Vibrating Zone-Drawing

AKIHIRO SUZUKI, TOSHIO SUGIMURA, TOSHIO KUNUGI

Department of Applied Chemistry and Biotechnology, Faculty of Engineering, Yamanashi University, 4-3-11 Takeda, Kofu 400-8511, Japan

Received 19 June 2000; accepted 22 October 2000

ABSTRACT: A continuous vibrating zone-drawing (CVZD) was applied to study the effect of vibration on the mechanical properties and superstructure of isotactic polypropylene fibers. The CVZD treatment was a new drawing method by which the fiber was continuously drawn at a rate of 0.5 m/min under vibration using the specially designed apparatus. The CVZD treatment was carried out in five steps at a drawing temperature of 150°C and a frequency of 100 Hz, and applied tensions increased step by step with processing in the range of 14.8 to 207 MPa. The obtained fiber had a birefringence of 0.0373, crystallinity of 62.4%, tensile modulus of 17.6 GPa, and tensile strength of 1.11 GPa. These values are higher than those of the continuous zone-drawn isotactic polypropylene fiber previous reported. The vibration added to the fibers during the zone-drawing was effective in developing amorphous orientation and improving the mechanical properties. © 2001 John Wiley & Sons, Inc. J Appl Polym Sci 81: 600–608, 2001

Key words: isotactic polypropylene fiber; continuous vibrating zone-drawing; drawing condition; mechanical properties; superstructure

INTRODUCTION

To date many studies have been carried out in the development of high-performance isotactic polypropylene (i-PP) with high modulus and tensile strength: Kunugi et al.[1,2] reported that the zone-annealed i-PP fiber had a storage modulus (E') of 21 GPa at room temperature, and that the film drawn at an extrusion draw ratio of 12 by coextrusion had $E' = 13$ GPa at room temperature; Wills et al.[3] studied the effect of molecular weight on the drawing behavior and structural characteristics of ultra high modulus products. They reported that the polymer with $\overline{M}_w = 181{,}000$ had the highest modulus of 18 GPa; Taraiya et al.[4] reported that the tensile modulus of a die-drawn i-PP increased with draw ratio and reached 16.4 GPa at a draw ratio of 19.5; Peguy and St. John Manley[5] showed that the films prepared by drawing dry gels of high molecular weight i-PP had a tensile modulus of 36 GPa and tensile strength of 1.03 GPa.

The axial elastic moduli of the i-PP crystals were reported by various investigators: a value of 45 GPa was reported by Sakurada et al.[6]; a value of 88 GPa was estimated by Fanconi and Rabolt,[7,8]; and a value of 25 GPa was theoretically calculated by Tashiro et al.[9] The gap between the achieved and theoretical modulus is considerably small when compared to that of semicrystalline polymers. The moduli of polymers with a high degree of crystallinity such as i-PP can be ex-

Correspondence to: A. Suzuki (E-mail: a-suzuki@ab11.yamanashi.ac.jp).

Journal of Applied Polymer Science, Vol. 81, 600–608 (2001)

pected to approach the theoretical values because of the existence of intercrystallinity in the polymers. The increase in modulus is attributed to an increase in the degree of crystal continuity.[10]

The i-PP crystallizes in three polymorphic forms: α-monoclinic, β-hexagonal,[11–13] and γ-orthorhombic crystal forms.[14,15] The α form is the most stable crystalline phase and can be easily obtained by crystallization from the melt or from solution.[3] The α form is further classified in two limiting modifications, α_1 and α_2.[16,17] The α_1 form is characterized by a statistical disorder like that described for the space group C2/c. The α_2-form is characterized by regularity of up- and down-positioning of the chains, as in the space group $P2_1/c$.

Jacoby et al.[18] studied the mechanical, thermal, and morphological characteristics of melt-crystallized isotactic polypropylene containing high levels of the β or pseudohexagonal crystalline form. They produced different levels of β-form crystallinity in the polymer by blending in low levels of quinacridone dye nucleating agent. They showed that dynamic mechanical measurements obtained on nonoriented specimens containing varying levels of β-form crystallinity showed an increase in the magnitude of the damping in the post-T_g region with increasing β content. High levels of the β form led to lower values of the modulus and yield stress, but led to higher values of the elongation at break and impact strength. Kalay et al.[19,20] studied the occurrence of the γ form in an injection-molded i-PP and reported that the γ form was associated with the pronounced molecular orientation.

We previously proposed various methods, such as zone-drawing/zone-annealing,[21–23] high-tension annealing,[24,25] continuous zone-drawing (CZD),[26–28] vibrating hot-drawing,[29] and vibrating zone-drawing[30] methods, which not only have already been applied to many polymers so as to improve their mechanical properties but were also then found to be effective in producing fibers with high modulus and high strength. To further improve the mechanical properties of fibers and to continuously draw fibers, the continuous vibrating zone-drawing (CVZD) method, in which fibers are continuously drawn under vibration, was proposed. In this drawing, it was expected that the vibration might draw out molecular chains together with heating and tension in a complex structure, thus weakening intermolecular forces such as van der Waals forces.

The purpose of this study was twofold: to produce high-modulus i-PP fibers using the CVZD method and to study the effect of the vibration on mechanical properties. The changes in the mechanical properties and microstructure during the treatments were investigated using dynamic viscoelasticity, differential scanning calorimetry, thermal mechanical analysis, and X-ray diffraction measurement. Finally, the results of this study are compared to those of our earlier study of the continuous zone-drawing on mechanical properties and microstructure.

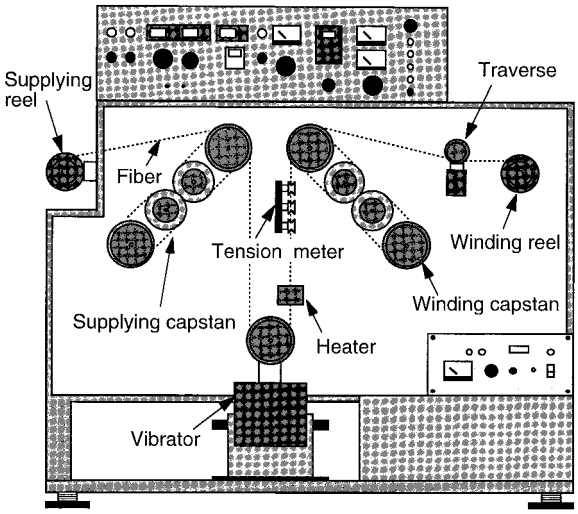

Figure 1 Scheme of apparatus used for continuous vibrating zone-drawing (CVZD).

EXPERIMENTAL

Material

The i-PP fibers were produced from commercial grade i-PP pellets (Idemitsu Petrochemical Co., Ltd.) by using a melt-spinning unit at a spinning temperature of 230°C. The pellet has $\overline{M_w}$ = 30,000 and $\overline{M_n}$ = 50,000. Its tacticity is highly isotactic at approximately 96%, which was determined by using nuclear magnetic resonance techniques. The samples were spun into monofilaments using a laboratory-scale melt extruder and take-up unit. The as-spun fibers had a diameter of 0.40 mm, degree of crystallinity of 44%, and a birefringence of 1.2×10^{-3}.

Apparatus for Continuous Vibrating Zone-Drawing

A schematic diagram of the apparatus used for the CVZD treatment is given in Figure 1. The apparatus is basically identical with an appara-

tus[28] using the CZD treatment reported previously, and a vibrator was mounted on the apparatus to apply vibration to the fiber during the drawing. The apparatus consists of supplying and winding reels, supplying and winding capstans, the vibrator, a temperature-controlled heater, a tension meter, and a traverse. The as-spun monofilament after unwinding from the supplying reel passes through the supplying capstan, the pulley attached on the vibrator, the temperature-controlled zone-heater, and the tension meter, and finally is wound on the winding reel after passing through the winding capstan and the traverse. The applied tension was generated by changing the ratio of the winding speed to the supplying speed.

Measurement

A draw ratio was determined in the usual way of measuring the displacement of ink marks placed 10 mm apart on the specimens prior to drawing. A birefringence was measured with a usual polarizing microscope equipped with a Berek compensator (Olympus Optical Co., Ltd.). The density of each fiber was measured with the flotation technique using a water and methanol mixture. An apparent mass crystallinity X_w was obtained using the relation

$$X_w = [d_c(d - d_a)]/[d(d_c - d_a)] \times 100 \qquad (1)$$

where d_c and d_a, the densities of the crystalline and amorphous phases, were 0.936 and 0.850 g/cm^3, respectively.[31,32] The density of amorphous polymer was assumed to be constant, independent of treatments.

The orientation factor of crystallites (f_c) was evaluated by using the method of Wilchinsky[33] from the wide-angle X-ray diffraction pattern. An amorphous orientation factor (f_a) was estimated from the measured birefringence (Δn), degree of crystallinity, and f_c using

$$\Delta n = X_v f_c \Delta n_c^\circ + (1 - X_v) f_a \Delta n_a^\circ \qquad (2)$$

where X_v is a volume fraction crystallinity, Δn_c°, the intrinsic crystallite birefringence, and Δn_a°, the intrinsic amorphous birefringence, were 0.0331 and 0.0468, respectively.[34]

Flat-plate wide-angle X-ray diffraction patterns for the fibers were obtained with a Rigaku X-ray generator. The radiation used was Ni-filtered CuK$_\alpha$ (wavelength 1.542 Å). An X-ray unit was operated at 36 kV and 18 mA. The sample-to-film distance was 40 mm. The fiber was wound on a frame in a parallel alignment and exposed to the X-ray beam from a 0.015-in.-diameter pinhole collimator for 3 h.

Differential scanning calorimetry (DSC) measurements were carried out by using a Rigaku DSC 8230C calorimeter. The DSC scans were performed over the temperature range from 25 to 180°C, using a heating rate of 10°C/min in a nitrogen gas atmosphere.

A thermal shrinkage was measured with a Rigaku SS-TMA at a heating rate of 5°C/min. The measurements were performed over the temperature range from 30 to 125°C. The specimens (15 mm long) were given a very small tension (5 g/cm^2) to stretch the specimen tightly.

Tensile properties were determined with a Tensilon tensile testing machine (Orientec Co.). The fiber was tested at a crosshead speed of 10 mm/min with a gauge length of 50 mm. The tensile modulus, tensile strength, and elongation at break were calculated from the stress–strain curves obtained at 23°C and 65% relative humidity.

Dynamic viscoelastic properties were measured at 110 Hz with a dynamic viscoelastometer VIBRON DDV-II (Orientec Co.). Measurement was carried out over a range of temperature from −15°C to about 150°C at a temperature interval of 2.5°C. During the measurement, the average heating rate was 2°C/min.

RESULTS AND DISCUSSION

Optimum Conditions for the CVZD

A significant improvement in the mechanical properties of crystalline polymers can be obtained by an increase in fraction of taut tie chains. The increase of the tie chains would be promoted by the conversion of an original spherulitic lamellar structure into an extended microfibrillar form. The optimum draw temperature to induce a pronounced morphological change and an increase in overall molecular orientation lies between the glass transition and the melting point.[35]

To study the effect of vibration during drawing on the drawability, crystallization, orientation, and mechanical properties, it is necessary to compare the data of the CVZD fibers with those of the fibers drawn without vibration. All conditions, except vibration, for the CVZD treatment are the

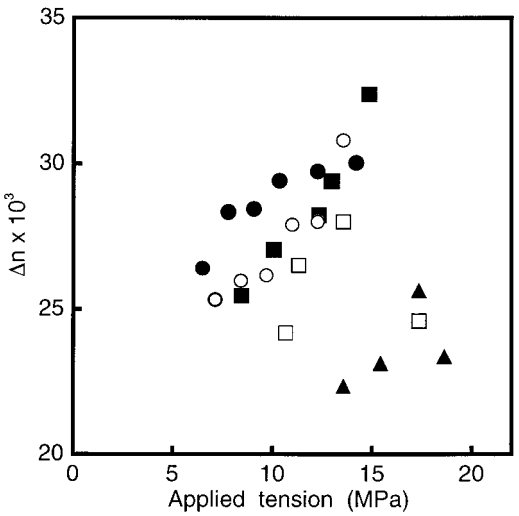

Figure 2 Relation between applied tension and birefringence (Δn) for CVZD-1 fibers drawn at various temperatures: (▲) T_d = 90°C; (□) T_d = 140°C; (■) T_d = 150°C; (○) T_d = 160°C; (●) T_d = 170°C.

same as the optimum conditions for the CZD treatment reported previously.[28]

To determine the optimum condition of vibration, the CVZD treatments were first carried out at variable frequencies between 50 and 200 Hz with the amplitudes between 0.05 and 0.1 mm. The preliminary experiments indicated that the optimum frequency and amplitude for adding vibration during drawing were 100 Hz and 0.1 mm.

Figure 2 shows the relation between the applied tension and the birefringence (Δn) of the fibers obtained under such conditions for the first step. The Δn values, except for those of the fibers drawn at 90 and 170°C, increase linearly with the applied tension, and the fiber drawn at 150°C under 14.8 MPa attains the highest value (0.0324), thus confirming that the optimum drawing temperature and applied tension for the first step (CVZD-1) of the CVZD treatment are the same as the optimum conditions for the first step (CZD-1) of the CZD treatment. Furthermore, it was found that the optimum conditions for other CVZD treatments were also the same as those in the case of the CZD treatment. The optimum conditions for the CVZD treatments of the i-PP fiber were tabulated and are presented in Table I. The microstructure and mechanical properties of the fiber obtained by drawing with and without vibration is discussed below.

The draw ratio (λ), Δn, degree of crystallinity (X_w), and orientation factors of the crystallite and amorphous phases (f_c and f_a, respectively) for the CVZD and CZD fibers are given in Table II. The values, except f_c, increase with an increase in the number of treatments. The crystallization at high orientation proceeds at a rate many times faster than that at low orientation and is promoted along the drawing direction.[36,37] Such crystal growth forms the crystalline bridges connecting longitudinally crystal regions and develops the amorphous orientation. The increases in Δn, X_w, and f_a values suggest that the amorphous chain is stretched and oriented highly by the evolution of crystallization along the drawing direction.

The Δn and f_a of the CVZD fiber at each step are slightly higher than those of the CZD fibers, but the X_w's of the CVZD fibers tend to be lower than those of the CZD fibers. In spite of the same drawing temperature and applied tension as in the CZD treatments, the CVZD fibers show a high degree of orientation and low degree of crystallinity. These results imply that the vibration prompts amorphous molecular chains to orient to the drawing direction, but that it inhibits the evolution of crystallization.

We studied the effect of vibrating poly(ethylene terephthalate) (PET) films being drawn on the molecular orientation using the FTIR microscope.[38] The FTIR microscope is equipped with a drawing apparatus developed in our laboratory, and the apparatus has a vibrator and a sample chamber that is capable of heating at a constant rate. The FTIR microscope with the drawing apparatus is capable of measuring the temperature dependence of the spectra for the films drawn with and without the vibration. The obtained spectra showed that a *trans*-isomer content of the fiber drawn with vibration was higher than that of the fiber drawn without the vibration, which revealed that the vibration during drawing was effective in arranging molecular chains in the drawing direction.

The f_c values of the CVZD-1 and CZD-1 fibers already attain high values close to unity. In spite

Table I Optimum Conditions for CVZD

Step	Applied Tension (MPa)
CVZD-1	14.8
CVZD-2	101.7
CVZD-3	192.2
CVZD-4	201.1
CVZD-5	207.0

Supplying speed: 0.5 m/min; drawing temperature: 150°C; frequency: 100 Hz; amplitude: 0.1 mm.

Table II Draw Ratio (λ), Birefringence (Δn), Degree of Crystallinity (X_w), and Orientation Factors of Crystallite and Amorphous Phases (f_c and f_a) for the CVZD and CZD Fibers

Step	λ	Δn ($\times 10^3$)	X_w (%)	f_c	f_a
CVZD-1	7.1	32.4	50.1	0.991	0.650
CVZD-2	9.1	33.2	60.1	0.994	0.716
CVZD-3	10.2	35.9	61.8	0.993	0.862
CVZD-4	11.4	36.9	61.6	0.994	0.911
CVZD-5	12.5	37.3	62.4	0.994	0.940
CZD-1	8.0	30.1	53.6	0.993	0.555
CZD-2	10.4	31.6	59.3	0.994	0.637
CZD-3	10.9	33.3	63.3	0.995	0.726
CZD-4	11.1	34.0	67.3	0.994	0.771
CZD-5	11.2	34.8	65.0	0.995	0.810

of the first step, the crystallites are demonstrated to readily orient to the drawing direction. The effect of the vibration on the degree of crystallite orientation is obscure.

Figure 3 shows the wide-angle X-ray diffraction patterns of the CVZD-1, CVZD-3, and CVZD-5 fibers. There are three strong equatorial reflections [(110), (040), and (130)] and two weak reflections [(060) and (220)]. Both the α_1 and α_2 forms have substantially identical X-ray spectra. However, although only reflections with $(h + k)$ even are allowed in the α_1 form, reflections with $(h + k)$ odd may be present in the α_2 form.[20] All reflections observed are reflections with $(h + k)$ even. It is known that the β form exhibits a strong equatorial reflection (300) at $2\theta = 16.10°$, and that the γ form[18] is observed (113) at $2\theta = 14.98°$ and (117) at 20.06°. However, no reflections resulting from the β and γ form are observed in Figure 3. Therefore, these wide-angle X-ray diffraction patterns show that the only α_1 form exists in the CVZD fibers.

Figure 4 shows DSC curves of the original and the CVZD fibers. The DSC curves show the presence of only one peak, which is displaced toward a slightly higher temperature with processing. The melting behavior of i-PP crystallized in different ways has been studied by several investiga-

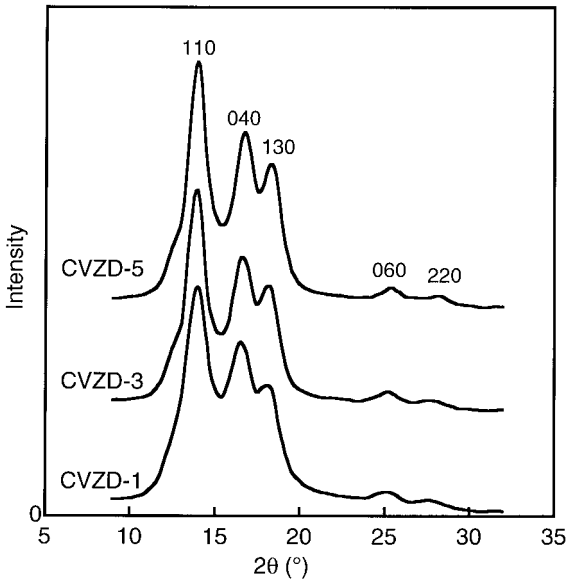

Figure 3 Wide-angle X-ray diffraction patterns of the CVZD-1, CVZD-3, and CVZD-5 fibers.

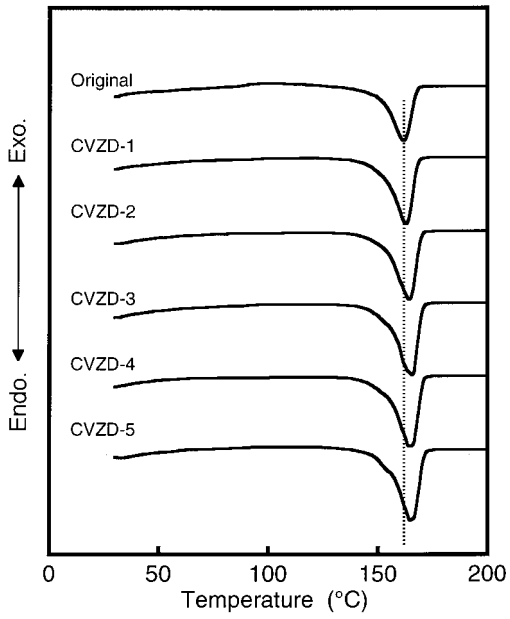

Figure 4 DSC curves of the original and CVZD fibers.

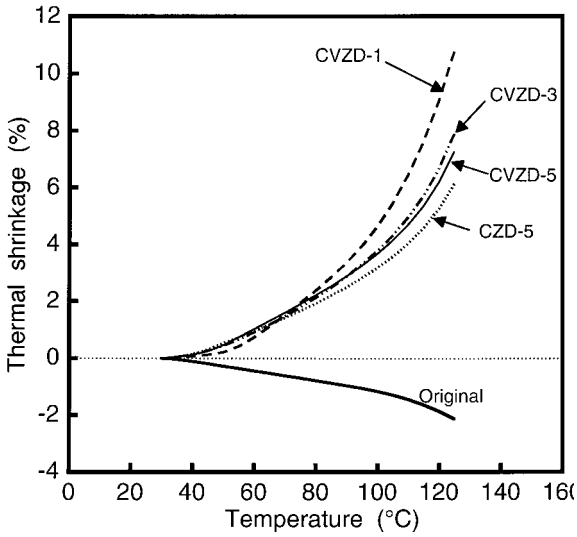

Figure 5 Temperature dependence of thermal shrinkage for the original and CVZD fibers.

tors.[39–45] A typical DSC curve has been multiple melting endotherm. The appearance of such multiple endotherms has been attributed to both the α_1 form and the α_2 form. The low endotherm peaking at about 160°C results from the melting of the α_1 form, and the high endotherm peaking above 170°C is attributed to the melting of the α_2 form.[42] Jacoby et al.[16–18] reported that the melting endotherm attributed to the melting of the β form was observed at about 150°C. No β and γ forms are detected in Figure 4. The melting peak of all fibers is located in the temperature range of 160 to 165°C. It means, therefore, that all melting peaks result from the melting of the α_1 form, which is substantiated by the wide-angle X-ray diffraction patterns.

Caldas et al.[46] showed that the low-temperature endotherm peaking at about 60°C shifted to higher temperature with an increase of annealing temperature and coalesced into the main melting endotherm in samples annealed at temperatures above 100°C. They attributed it to the melting of an imperfect crystalline morphology. On the other hand, no low-temperature endotherm is observed in the DSC thermograms of the CVZD fibers, as shown in Figure 4, although a trace of shoulder is observed on the low-temperature side of its peak. The appearance of the shoulder is probably ascribed to the melting of the imperfect crystalline morphology.

Figure 5 shows the temperature dependence of thermal shrinkage for the original, CVZD-1, -3, -5, and CZD-5 fibers. The development of the thermal shrinkage during heating is associated with the chain coiling in the oriented amorphous regions[47] and dependent on both f_a and degree of crystallinity. The original fiber expands gradually above 30°C. On the other hand, the CVZD and CZD fibers shrink above 30°C as the temperature increases. The CVZD-1 fiber shrinks rapidly above 80°C, but the CVZD-3, -5, and CZD-5 fibers shrink moderately above the 100°C with increasing temperature. There is a slight difference in the shrinking behavior between the CVZD-5 and CZD-5 fibers; between the drawings with and without vibration. This difference is attributed to a crosslink density of the physical network built up by crystallites and the degree of amorphous orientation. Therefore, the physical network in the CVZD-5 fiber was insufficient for constraint of the thermal shrinkage because of its slightly low X_w and high amorphous orientation when compared to that of the CZD fiber, which implies that the CVZD fibers show the higher degree of orientation and lower degree of crystallinity.

Mechanical Properties of the CVZD Fibers

Tensile properties of the CVZD and the CZD fibers are given in Table III. The tensile modulus and strength increase stepwise with increased processing. The resulting CVZD-5 fiber has a tensile modulus of 17.6 GPa and a tensile strength of 1.11 GPa. The tensile properties of the CVZD-5 fiber are notably higher than those of the CZD-5 fiber. This modulus is 39.1% of the axial elastic modulus,[6] 45 GPa, of the i-PP crystals. Figure 6 shows the relation between λ and the tensile modulus of the CVZD fibers. The modulus increases linearly up to a high draw ratio with increasing λ. Such a linear relation was previously reported by several authors.[4,5,48]

Figure 7 shows the temperature dependence of the tan δ for the fibers. In common with several other partially crystalline polymers, i-PP exhibits three relaxation regions labeled α, β, and γ, respectively.[49–51] Although α and β relaxations are observed in Figure 7, there is no γ relaxation over the temperature range measured in the present study because the γ relaxation is located at -50°C. The original fiber shows the α and β relaxations, although the CVZD fibers show the α relaxation and a trace of the β relaxation. The occurrence of β relaxation is considered to be attributed to the onset of chain mobility in the amorphous phase (i.e., glass transition), and the α relaxation can be identified as a c-shear relax-

Table III Tensile Modulus, Tensile Strength, and Elongation at Break for the CVZD and CZD Fibers

Step	Tensile Modulus (GPa)	Tensile Strength (GPa)	Elongation at Break (%)
CVZD-1	6.9	0.79	31.8
CVZD-2	10.9	1.06	18.6
CVZD-3	13.3	1.08	15.6
CVZD-4	15.2	1.08	13.6
CVZD-5	17.6	1.11	12.8
CZD-1	6.6	0.69	30.8
CZD-2	7.3	0.87	24.0
CZD-3	11.8	0.91	14.6
CZD-4	13.7	1.08	14.0
CZD-5	14.7	0.90	10.4

ation process (crystalline transition; i.e., a c-slip process). The trace of β relaxation shifts to a higher temperature and decreases in its peak height with processing, and finally no β relaxation appears in the tan δ curve of the CVZD-5 fiber. The changes in position and in profile of the β relaxation with processing indicate that the molecular mobility in the amorphous phase is restricted by the physical network with a higher degree of crosslink density. Wills et al.[3] studied the dynamic mechanical behavior of ultra high modulus material obtained for $\overline{M_w}$ in the range of 180,000 and 400,000. They show that the absence of the β relaxation in the drawn sample is primarily attributable to the orientation of the intercrystalline material. Therefore, the vibration applied to the fiber being drawn was confirmed to be effective in improving the mechanical properties.

Figure 8 shows the temperature dependence of the storage modulus (E') of the original fiber, CVZD fibers, and CZD-5 fiber. In each case the E' decreases as the temperature increases, but decreases much more rapidly in the temperature range of 20 to 50°C. The rapid decrease in E' is attributed to the β relaxation. Above the glass transition, the E' decreases linearly with temperature, but no rapid decrease resulting from the α relaxation is observed. The difference in E' between the CVZD-5 and CZD-5 fibers is large at low temperatures, decreasing with increasing temperature, but the E'-temperature curves of the CVZD-5 and the CZD-5 fibers overlap each other above 90°C.

The dynamic viscoelastic properties of the CVZD-5 fiber can be measured up to 150°C, that is, the temperature began to melt crystallites, as

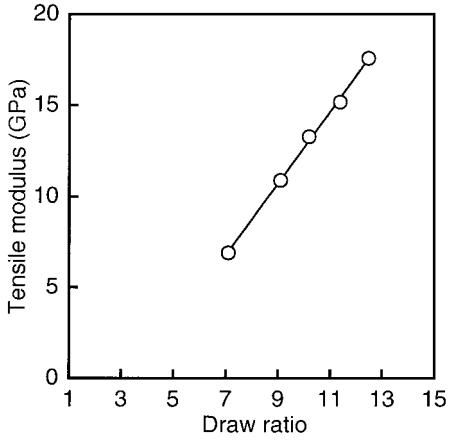

Figure 6 Relation between draw ratio and tensile modulus.

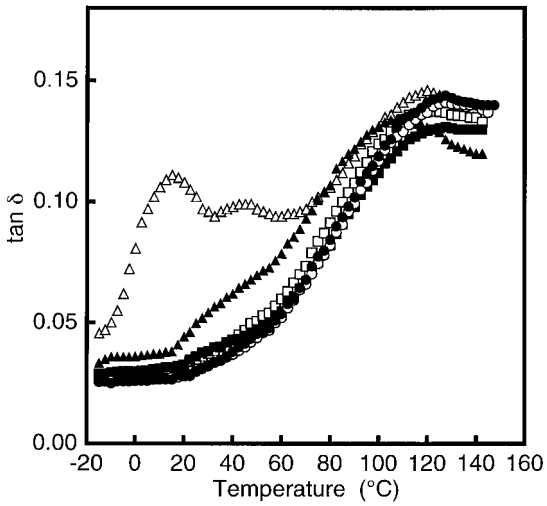

Figure 7 Temperature dependence of tan δ for the original, CZD, and CZA fibers: (△) original; (▲) CVZD-1; (□) CVZD-2; (■) CVZD-3; (○) CVZD-4; (●) CVZD-5.

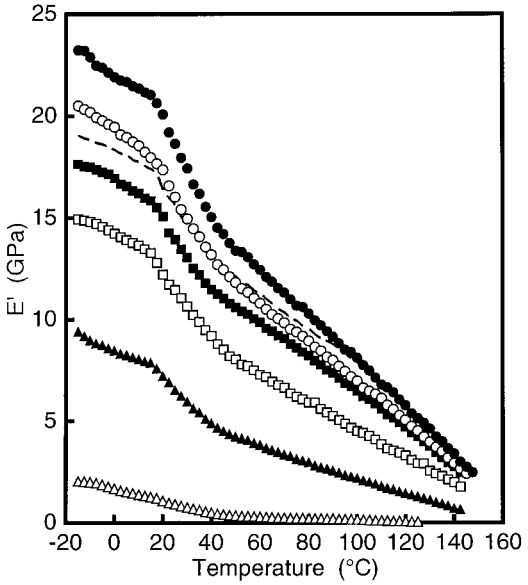

Figure 8 Temperature dependence of storage modulus (E') for the original fiber, CVZD fibers, and CZD-5 fiber: (△) original; (▲) CVZD-1; (□) CVZD-2; (■) CVZD-3; (○) CVZD-4; (●) CVZD-5; broken line, CZD-5.

shown in Figure 9, illustrating the temperature dependence of the E' and the DSC curve for the CVZD-5 fiber. For semicrystalline polymers such as PET and nylon, the measurement of the dynamic viscoelastic properties could not be carried out up to temperatures close to their melting points. For the continuous zone-annealed PET fiber[26] reported previously, its dynamic viscoelastic properties were measured up to about 210°C,

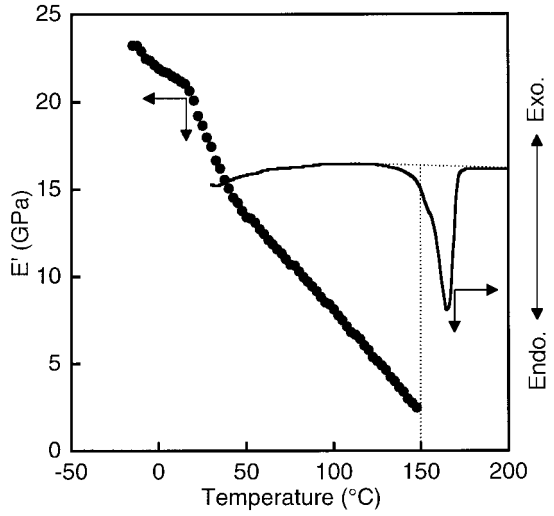

Figure 9 Temperature dependence of storage modulus (E') and DSC curve for the CVZD-5 fiber.

which was about 40°C lower than its melting point. The high thermostability implies that the intercrystalline bridges of the CVZD-5 fiber longitudinally connect the crystal regions.[52]

CONCLUSIONS

The continuous vibrating zone-drawing (CVZD) method has been applied to isotactic polypropylene fibers so as to improve their mechanical properties. The results allow the following conclusions:

1. The degree of crystallinity increased to 62.4% by the CVZD treatments. The orientation factor of crystallites increased to 0.991 with only the first CVZD treatment. At the same time, the amorphous orientation factor increased stepwise with processing.
2. The CVZD-5 fiber was characterized by a tensile modulus of 17.6 GPa and a tensile strength of 1.11 GPa. The dynamic viscoelastic properties of the CVZD-5 fiber can be measured up to the temperature that begins to melt crystallites. The dynamic mechanical behavior implies that the intercrystalline bridges longitudinally connect the crystal regions. The CZD-5 fiber, which was prepared under the same conditions (except vibration) as those of the CVZD treatments, had a tensile modulus of 14.7 GPa and tensile strength of 0.90 GPa. The difference in the mechanical properties between the CVZD and CZD fibers is attributed to the vibration during drawing, which suggests that the vibration has a strong tendency to orient molecular chains to the drawing direction, but inhibit crystallization.

REFERENCES

1. Kunugi, T.; Ito, T.; Hashimoto, M.; Ooishi, M. J Appl Polym Sci 1983, 28, 179.
2. Kunugi, T.; Yoneyama, Y.; Porter, R. S. J Appl Polym Sci 1990, 41, 155.
3. Wills, A. J.; Capaccio, G.; Ward, I. M. J Polym Sci Polym Phys Ed 1980, 18, 493.
4. Taraiya, A. K.; Unwin, A. P.; Ward, I. M. J Polym Sci Polym Phys Ed 1988, 26, 817.

5. Peguy, A.; St. John Manley, R. Polym Commun 1984, 25, 39.
6. Sakurada, I.; Ito, T.; Nakamae, K. J Polym Sci 1966, 15, 75.
7. Rabolt, J. F.; Fanconi, B.; J Polym Sci Polym Lett Ed 1977, 15, 121.
8. Fanconi, B.; Rabolt, J. F. J Polym Sci Polym Phys Ed 1985, 23, 1201.
9. Tashiro, K.; Kobayashi, M.; Tadokoro, T. Macromolecules 1977, 10, 731.
10. Uniwin, A. P.; Bower, D. I.; Ward, I. M. Polymer 1990, 31, 882.
11. Fujiwara, Y.; Goto, T.; Yamashita, Y. Polymer 1987, 28, 1253.
12. Tjong, S. C.; Shen, J. S.; Li, R. K. Y. Polymer 1996, 37, 2309.
13. Dorset, D. L.; McCourt, M. P.; Kopp, S.; Schumacher, M.; Okihara, T.; Lotz, B. Polymer 1998, 39, 6331.
14. Brücker, S.; Meille, S. V. Nature 1989, 340, 455.
15. Meille, S. V.; Brücker, S.; Porzio, W. Macromolecules 1990, 23, 4114.
16. Hikosaka, M.; Seto, T. Polym J 1973, 5, 111.
17. Napolitano, R. J Polym Sci Polym Phys Ed 1990, 28, 139.
18. Jacoby, P.; Bersted, B. H.; Kissel, W. J.; Smith, C. E. J Polym Sci Polym Phys Ed 1986, 24, 461.
19. Kalay, G.; Allan, P.; Bevis, M. J. Polymer 1994, 35, 2480.
20. Kalay, G.; Zhong, Z.; Allan, P.; Bevis, M. J. Polymer 1996, 37, 2077.
21. Kunugi, T.; Suzuki, A.; Hashimoto, M. J Appl Polym Sci 1981, 26, 1951.
22. Suzuki, A.; Kohno, T.; Kunugi, T. J Polym Sci Polym Phys Ed 1998, 36, 1731.
23. Suzuki, A.; Kuwabara, T.; Kunugi, T. Polymer 1998, 39, 4235.
24. Suzuki, A.; Endo, A. Polymer 1997, 38, 3085.
25. Suzuki, A.; Murata, H.; Kunugi, T. Polymer 1998, 39, 1351.
26. Suzuki, A.; Sato, Y.; Kunugi, T. J Polym Sci Polym Phys Ed 1998, 36, 473.
27. Suzuki, A.; Chen, Y.; Kunugi, T. Polymer 1998, 39, 5335.
28. Suzuki, A.; Sugimura, T.; Kunugi, T. Kobunshi Ronbunshu 1997, 54, 351.
29. Kunugi, T.; Suzuki, A. J Appl Polym Sci 1996, 62, 713.
30. Kunugi, T.; Chida, K.; Suzuki, A. J Appl Polym Sci 1998, 67, 1993.
31. Natta, G.; Corradini, P. Nuovo Cimento Soc Ital Fis Suppl 1960, 15, 40.
32. Natta, G. J Polym Sci 1955, 16, 143.
33. Wilchinsky, Z. W. J Appl Phys 1963, 30, 792.
34. Samuels, R. J. J Polym Sci Part A Polym Chem 1965, 3, 1741.
35. Taylor, W. N., Jr.; Clark, E. S. Polym Eng Sci 1978, 18, 518.
36. Peszkin, P. N.; Schultz, J. M.; Lin, J. S. J Polym Sci Polym Phys Ed 1986, 24, 2592.
37. Murthy, N. S.; Bray, R. G.; Correale, S. T.; Moore, R. A. F. Polymer 1995, 36, 3863.
38. Suzuki, A.; Sugimura, T.; Kunugi, T. J Appl Polym Sci, submitted.
39. Hsu, C. C.; Geil, P. H.; Miyaji, H.; Asai, K. J Polym Sci Polym Phys Ed 1986, 24, 2379.
40. Guerra, G.; Petraccone, V.; Corradini, P.; DeRosa, C.; Napolitano, R.; Pirozzi, B. J Polym Sci Polym Phys Ed 1984, 22, 1029.
41. Yadav, Y. S.; Jain, P. C. Polymer 1986, 27, 721.
42. Awaya, H. Polymer 1988, 29, 591.
43. Paukkeri, R.; Lehtinen, A. Polymer 1993, 34, 4075.
44. Paukkeri, R.; Lehtinen, A. Polymer 1993, 34, 4083.
45. Vleeshouwers, S. Polymer 1997, 38, 3213.
46. Caldas, V.; Brown, G. R.; Nohr, R. S.; MacDonald, J. G.; Raboin, L. E. Polymer 1994, 35, 899.
47. Wilson, M. P. W. Polymer 1974, 15, 277.
48. Vittoria, V.; De Candia, F.; Capodanno, V. J Polym Sci Polym Phys Ed 1986, 24, 1009.
49. Boyd, R. H. Polymer 1985, 26, 323.
50. Jourdan, C.; Cavaille, J. Y.; Perez, J. J Polym Sci Polym Phys Ed 1989, 27, 2361.
51. Read, B. E. Polymer 1989, 30, 1439.
52. Gibson, A G.; Davies, G. R.; Ward, I. M. Polymer 1978, 19, 683.